



## **ASSESSMENT OF STATE VARIABLE CONTROL APPROACH FOR ENERGY MANAGEMENT OF HYBRID ENERGY SYSTEM FOR ELECTRIC VEHICLES**

**Neeraj Kumar Bahuguna**, Department of Electrical Engineering, College of Technology, G.B. Pant University of Agriculture & Technology, Pantnagar, Uttarakhand, India.

**Rajiv Singh**, Associate Professor, Department of Electrical Engineering, College of Technology, G. B. Pant University of Agriculture and Technology, Pantnagar, Uttarakhand, India.

### **ABSTRACT**

Energy Management System (EMS) is crucial for Electric Vehicles (EVs) to optimize their performance, enhance efficiency, and ensure the durability of the vehicle's energy storage system. It is instrumental in maximizing battery life by monitoring State of Charge (SOC) and temperature, thereby maintaining optimal battery performance. Additionally, the EMS efficiently manages power flows within the vehicle, controls the power-train, and adjusts energy usage based on driving conditions to maximize their range. The area of power and energy management in EVs is relatively new and encompasses many disciplines. Managing EVs with multiple energy storage systems presents challenges such as handling energy consumption, determining optimal power distribution, and establishing interfaces between energy systems to meet propulsion and auxiliary load requirements. This paper aims to check the efficacy of proposed state variable approach towards addressing these challenges on a hybrid energy system for EVs comprising a Li-ion battery, a supercapacitor and a solar-PV panel. From the obtained results, it was concluded that the state variable approach was capable of successfully and efficiently regulating the power output from the different sources and can be used for energy management in EVs.

### **Keyword:**

Electric Vehicle, Energy management, Hybrid energy system, State variable approach

### **I. Introduction**

In the past years, transportation industry has increasingly focused on creating efficient and eco-friendly propulsion systems, leading to the realization of hybrid EVs. Presently, PV array is utilized across various modes of transportation, including cars, buses, tramways, trains, and aircraft. They offer efficient power generation, reduced noise, and nearly zero emissions compared to traditional internal combustion engines [1]-[3]. As part of the initial steps toward greener transportation the manufacturers of EVs are transitioning from conventional energy systems to hybrid systems involving PV arrays and battery storage. Improving the dynamics and power density of PV arrays necessitates their hybridization with emerging energy storage technologies like lithium-ion batteries or supercapacitors. The hybrid approach optimizes PV array system performance, enhancing fuel economy and overall efficiency by allowing the batteries/supercapacitors to share the load [4], [5]. Effective optimization is achieved through an energy management strategy (EMS), which allocates power distribution amongst various energy generators while ensuring the operation of each component within tolerable limits. Moreover, the efficient EMS design aims in minimizing the harmful impact of factors such as temperature on the state of health (SOH) of hybrid energy system.

In this paper, state-variable approach has been proposed for managing the flow of energy in a hybrid energy system comprising a solar-PV panel, a Li-ion battery and a super-capacitor designed for EVs. The proposed approach considers the battery and super-capacitor state-of-charge (SOC) and over-all system efficiency for analysing the performance of EMS.

The analysis involves experimental validation through simulation of state variable approach-based EMS for a hybrid power system containing PV array, Li-ion battery and super-capacitor utilizing standard parameters of accuracy. The paper's primary contribution lies in providing performance evaluation of state variable EMS strategies for a hybrid energy system designed for EVs. This



evaluation considers the impact of proposed EMS on overall efficiency and system life cycle. This paper is organized as follows: introduction in presented section 1 is followed by review of literature about various energy management strategy used in EVs. Material and methods are presented in section 3 describing the mathematical modelling of each component used in this experimental analysis. Result and discussions are presented in section 4; while the conclusion of the research is presented in section 5.

## II. Literature Review

Literature review presented in this section is performed to highlight the achievements of various research works carried out in the past towards optimizing the performance of developed EMS strategies. A few important works amongst them are listed below:

*Aouzellag et al., 2015* focused on developing an advanced power management strategy for Fuel Cell/Ultracapacitor HEVs. Using state-flow blocks in Matlab/Simulink, they elaborated on a control strategy to efficiently distribute power between any two energy sources. Their approach aimed towards minimizing the FC power demand transitions thereby extending its lifespan. Besides, they also introduced an improved EMS for FC/UC HEVs. The control of the UC converter was optimized to maintain the DC bus voltage constant via current mode control, which also regulated UC current. Simulation results using a presented drive cycle demonstrated the potential of the proposed strategy to enhance cell durability and extended FC lifespan.

*Alloui et al., 2017* presented a comparative study between rule-based and frequency separation EMS in HEVs that utilized FC as the primary energy source and batteries for power peaks during acceleration and braking energy capture. The comparative analysis between frequency separation and rule-based strategies revealed their complementary nature. The frequency separation strategy offered good dynamic performance for the FC but disregarded its power limits, whereas the rule-based strategy-imposed power limits on the FC but lacked dynamic performance.

*Smith et al., 2018* introduced specific hybrid electric bus, and a new fuzzy rule-based energy EMS to determine the torque during acceleration and cruise events was proposed. Using simulation with a validated vehicle model and the MLTB drive cycle, the proposed strategy showed a 2.2% cumulative fuel consumption reduction compared to the existing EMS. This indicated the potential of the proposed strategy to reduce fuel consumption and emissions in hybrid electric buses.

*Sankarkumar and Natarajan., 2021* addressed the crucial role of the EMS in EVs, which facilitated smooth energy transfer from the power drive to the vehicle's wheels. Hybridization, coupled with efficient EM strategies, aimed to optimally utilize energy storage systems, improve performance and efficiency, extend drive range, and reduce battery size. Despite numerous articles in the literature on hybrid energy storage systems (HESS) and EM techniques, a comprehensive review on HESS configurations, various EM strategies used in EVs, and performance evaluation of EM strategies for HESS configurations had been lacking. The proposed EMS in this research aims towards filling this research gap.

## III. Material and methods

In this section the mathematical models of various components used for creating the hybrid energy system as depicted in the figure 1 below are presented.

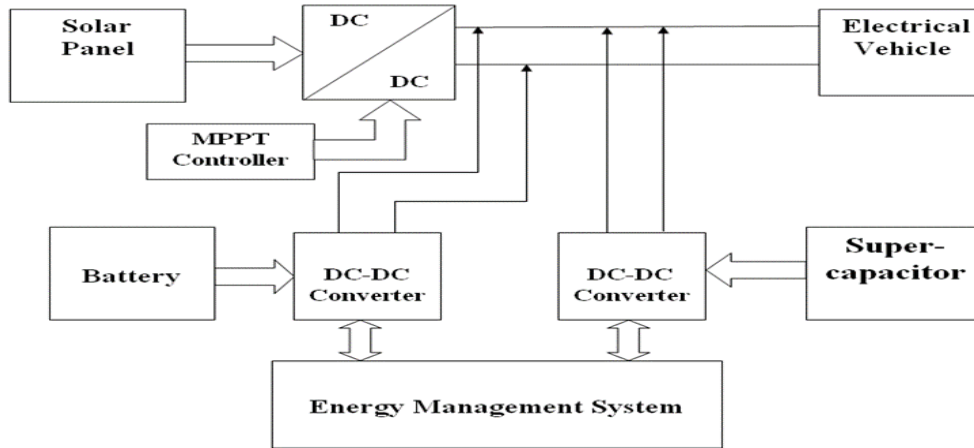


**Fig. 1 Block diagram of hybrid energy system with EMS.**

The mathematical model of each component of the hybrid energy system is explained as follows:

### 3.1 Model of PV array

Solar cells generate electricity by the help of sunlight, utilizing semiconductor materials like silicon or cadmium telluride etc. Mathematical modeling of PV array involves a set of equations or mathematical representations that describe the behavior and performance of the PV system under different conditions. This model is useful in the assessment of the PV array performance in terms of electrical energy generation in response to various environmental aspects and operational factors [6].

Fig. 2 depicted below represents the equivalent circuit diagram of a PV cell. Module Photo current is described by equation (1).

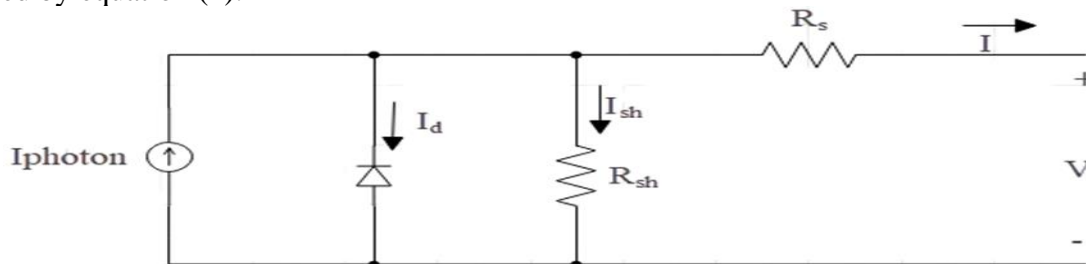


**Fig. 2 Equivalent circuit of PV cell**

$$I_{\text{photon}} = [I_{SC} + k_I(T - 298)] \times \frac{I_r}{1000} \quad (1)$$

Where,  $I_{\text{photon}}$  is photo current (A);  $I_{SC}$  is short circuit current (A);  $k_I$  is short circuit current of cell at 25°C and 1000 W/m<sup>2</sup> and T is operating temperature (K);  $I_r$  is solar irradiation (W/m<sup>2</sup>)

Module reverse saturation current  $I_{rs}$  is described by equation (2)

$$I_{rs} = \frac{I_{sc}}{[\exp(\frac{qV_{oc}}{N_s K n T}) - 1]} \quad (2)$$

where, q is electron charge which is 1.6 × 10<sup>-19</sup>C;  $V_{oc}$  is open circuit voltage (V);  $N_s$  is number of cells connected in series; n is ideality factor of the diode; k is Boltzmann's constant which is 1.38 × 10<sup>-23</sup>J/k.

The diode I-V characteristics is defined by equations (3) and (4)

$$I_{\text{diode}} = I_o \left[ \exp\left(\frac{V_d}{V_T}\right) - 1 \right] \quad (3)$$

Where,  $I_{\text{diode}}$  is the diode current,  $I_o$  is diode saturation current,  $V_d$  is diode voltage (V),  $V_T$  is terminal voltage (V).

$$V_T = \frac{kT}{q} \times n \times N_{\text{cell}} \quad (4)$$

where,  $N_{\text{cell}}$  is the number of series connected cells in a module

The table 1 shows the PV array design parameters used in this research work.

**Table 1: Design specification of PV array**

Design specification	Values
Parallel string	2
Series connected modules per string	1
Cell per module ( $N_{cell}$ )	72
Open circuit voltage (V)	44.7
Short circuit current (A)	8.78
Temperature coefficient of $V_{oc}$ (%/°C)	-0.4051
Temperature coefficient of $I_{sc}$ (%/°C)	0.075604
Voltage at maximum power point (V)	36.1
Current at maximum power point (A)	8.31

### 3.2. Super-capacitor (SC) model

The SC is an energy storage device known for its high-power density, making it valuable in certain applications. Unlike batteries, SC has lower energy density but higher power density. The mathematical model of SC is based on the simple equivalent circuit depicted in Fig. 3 [7].

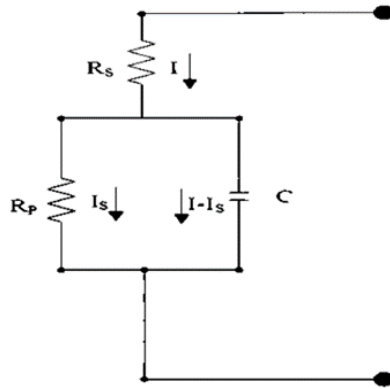


**Fig. 3: Electrical equivalent circuit of SC**

The SCs output voltage is expressed in equation 5

$$V_{Supercap} = \frac{N_s Q_T d}{N_p N_e \epsilon \epsilon_0} + \frac{2N_e N_s RT}{F} \text{Sinh}^{-1} \left( \frac{Q_T}{N_p N_e^2 A_i \sqrt{8RT \epsilon \epsilon_0 C}} \right) \quad (5)$$

where,  $A_i$  is Interfacial area between electrodes and electrolyte ( $m^2$ ),  $I_{sc}$  is SC current (A),  $V_{sc}$  is SC voltage (V),  $C_T$  is total capacitance (F),  $R_{sc}$  is Total resistance (ohms),  $C$  is molar concentration ( $mol/m^3$ ),  $R$  is molecular radius (m),  $F$  is Faraday's constant,  $N_e$  is the number of layers of electrodes,  $N_A$  is Avogadro constant,  $N_p$  is the number of parallel SC,  $N_s$  is Number of series SC,  $Q_T$  is Electric charge (C),  $R$  is Ideal gas constant,  $d$  is Molecular radius,  $T$  is Operating temperature (K),  $E$  is Permittivity of material and  $\epsilon_0$  is Permittivity of free space

The modeling parameters of SC are presented in table 2 below:

**Table 2: Design specification of SC**

Design specification	Values
Rated capacitance (F)	15.6
Equivalent DC series resistance(ohm)	0.150
Rated voltage(V)	290.6
Number of series capacitance	2
Number of parallel capacitance	5

Li-ion battery is modeled on the basis of equivalent circuit drawn below and the equations (6) and (7) representing its charging and discharging characteristics respectively [8].

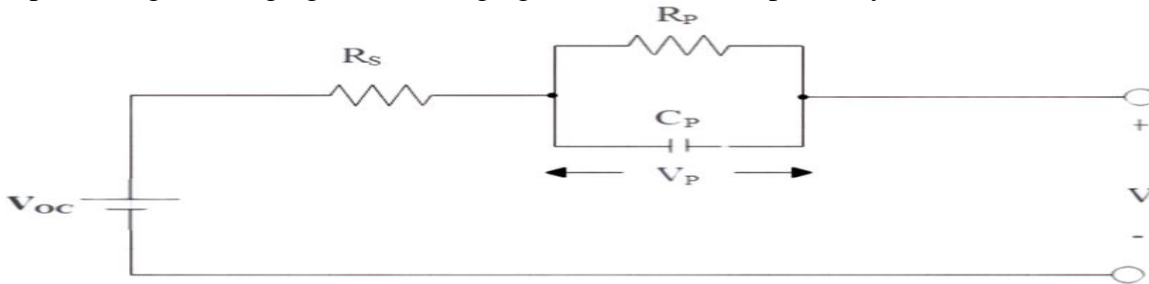


**Fig. 4: Electrical circuit model of Li-ion battery.**

**For charge model ( $I^0 > 0$ ):**

$$F_1(it, I^0, I) = E_0 - K \frac{Q}{Q - it} I^0 - K \frac{Q}{Q - it} it + A.Exp(-B.it) \quad (6)$$

**For discharge model ( $I^0 < 0$ ):**

$$F_1(it, I^0, I) = E_0 - K \frac{Q}{0.1Q + it} I^0 - K \frac{Q}{Q - it} it + A.Exp(-B.it) \quad (7)$$

Where,  $E_0$  is constant voltage in V,  $Exp(s)$  is exponential zone dynamics in V,  $Sel(s)$  is battery mode,  $Sel(s)$  is 0 (during battery discharge),  $Sel(s)$  is 1 (during battery charging),  $K$  is polarization constant in V/Ah,  $I^0$  is low-frequency current dynamics in A,  $I$  is battery current in A,  $it$  is extracted capacity in Ah,  $Q$  is maximum battery capacity in Ah,  $A$  is exponential voltage in V and  $B$  is exponential capacity in  $Ah^{-1}$ .

The table 3 below shows the values of different parameters used for modeling of the Li-ion battery:

**Table 3: Parameter specification of Li-ion battery**

Design specification	Values
Nominal voltage(V)	48
Rated capacity(Ah)	343.75
Initial SOC (%)	65
Battery response time(s)	1
Maximum capacity(Ah)	300
Cut off voltage(V)	36

### 3.4. Modeling of converters

Converters are essential components that help optimize energy flow, improve energy efficiency, and ensure the stability and reliability of power systems. There are several types of converters used in EMS, each with its specific function and characteristics (*Ehsani et. al. 1997*). The models of buck and boost converters used with PV arrays are depicted in Fig. 5 and Fig. 6 respectively.

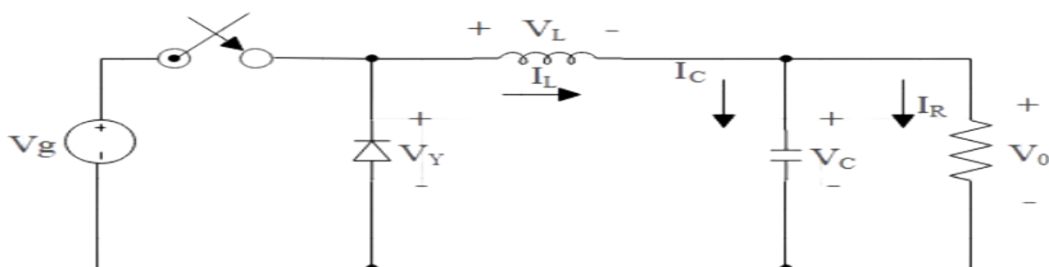


**Fig. 5: Schematic diagram of buck converter**

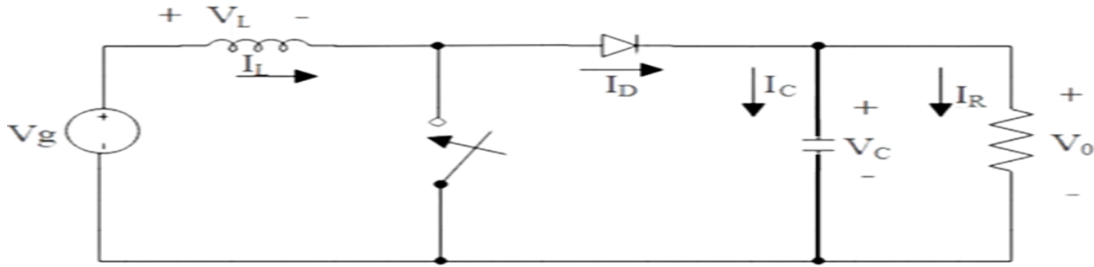


**Fig. 6: Schematic diagram of boost converter**

### 3.5. Electric drive model

In this work, BLDC drive system is used for representing the EV. The back emf characteristics of BLDC are trapezoidal. Trapezoidal back EMF" indicates represents that the mutual inductance between the stator and rotor has a trapezoidal configuration. Instead of using d-q axis two phase variables, more appropriate a-b-c three phase variables are used in creating the BLDC model. A few assumptions such as neglecting magnetic circuit saturation, assuming equal and constant stator resistance, self-inductance, and mutual inductance across all phases, the elimination of hysteresis and eddy current losses, and considering all semiconductor switches to be ideal are also taken for creating the model. The Phase voltage equations of BLDC motor are represented by equation 8 to 14:

$$V_a = Ri_a + (L - M) \frac{di_a}{dt} + E_a \tag{8}$$

$$V_b = Ri_b + (L - M) \frac{di_b}{dt} + E_b \tag{9}$$

$$V_c = Ri_c + (L - M) \frac{di_c}{dt} + E_c \tag{10}$$

Torque equations are each phase of BLDC motor are given by equations (11)-(14):

$$T_a = K_t \cdot i_a \cdot f(\phi_e) \tag{11}$$

$$T_b = K_t \cdot i_b \cdot f\left(\phi_e - \frac{2\pi}{3}\right) \tag{12}$$

$$T_c = K_t \cdot i_c \cdot f\left(\phi_e - \frac{4\pi}{3}\right) \tag{13}$$

The electromagnetic torque is

$$T = T_a + T_b + T_c \tag{14}$$

### 3.6 State variable control (SVC) strategy

SVC for a PV array, Li-ion battery, and SC-based hybrid energy system is a control approach that uses a set of predefined states and transitions between the states to efficiently manage the operation of a system. In this context, the states represent different operating modes or conditions of the hybrid energy system, and transitions between states dictate the system response towards changing conditions, load demand, and available energy sources. Fig. 7 depicts the block diagram of SVC based on SVC control strategy when PV array operated, fig.8 represents the operation of the control system when battery is operated.

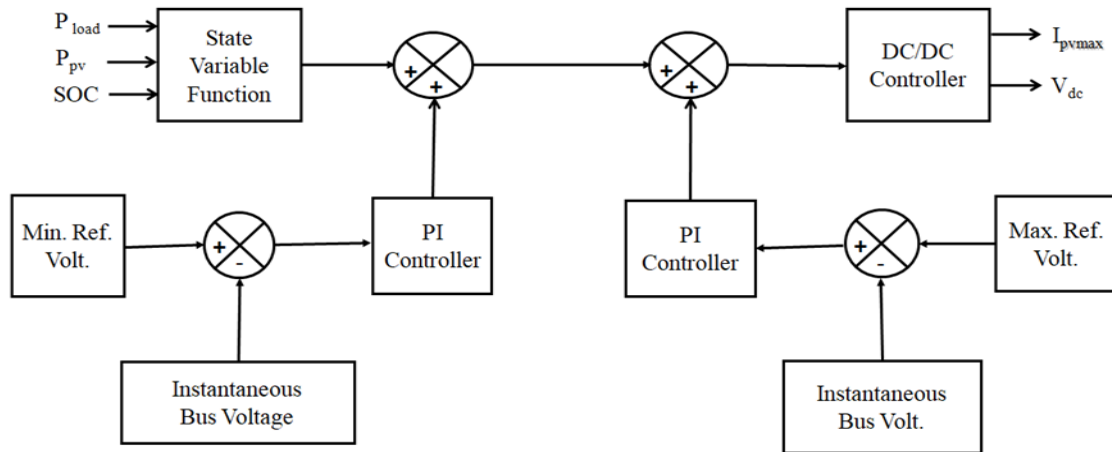


**Fig. 7: Block diagram of SVC during PV array operation.**

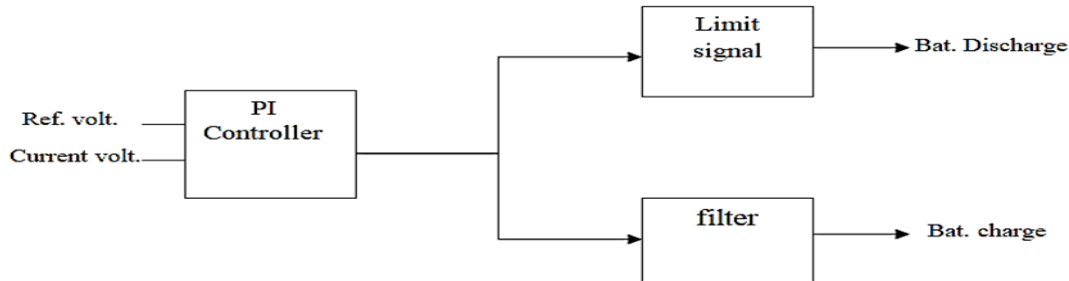


**Fig. 8: Block diagram of SVC during battery operation.**

The state transitions are typically governed by a control algorithm that considers system parameters, load demand, energy generation from the PV array, and the SOC of the battery and SC. When solar energy is abundant and the load demand is low, the system will bring the PV array into "Charging Battery" mode while directing excess energy towards the battery for charging, while during the periods of high load demand or when the PV array's output is insufficient, the control strategy will switch to the "Discharging Battery" mode, utilizing the energy stored in the battery to meet the load. The SC will be used for short-duration high-power bursts, so the control strategy will involve transitions to "Discharging SC" mode when rapid power delivery is required.

The proposed SVC approach comprises eight states, as illustrated in Table 4. The power output of the PV array is determined based on the range of the battery's SOC and the power required by the load ( $P_{load}$ ). Table 5 depicts the reference values used for control algorithms of state variable control strategy.

**Table 4: States of state variable control strategy.**

If SOC Normal & $P_{load} > P_{pvmin}$	State = 1	$P_{pv} < P_{pvmin}$
If SOC Normal & $P_{load} > P_{pvmax}$	State = 2	$P_{pv} > P_{pvopt}$
If SOC High & $P_{load} \geq P_{pvmax}$	State = 3	$P_{pv} = P_{pvmax}$
If SOC Normal & $P_{load} < P_{pvopt}$	State = 4	$P_{pv} = P_{pvmax}$
If SOC Normal & $P_{load} \in [P_{pvopt}, P_{pvmax}]$	State = 5	$P_{pv} = P_{pvopt}$
If SOC Normal & $P_{load} \geq P_{pvmax}$	State = 6	$P_{pv} = P_{pvmax}$
If SOC Low & $P_{load} < P_{pvmax}$	State = 7	$P_{pv} = P_{load}$
If SOC Low & $P_{load} \geq P_{pvmax}$	State = 8	$P_{pv} = P_{pvmax}$

**Table 8: Reference values of variables used in EMS approaches.**

S.No.	System State	Reference Value
1.	$SOC_{min}$	60
2.	$SOC_{nom1}$	85

3.	$SOC_{nom2}$	60.1
4.	$SOC_{max.}$	90
5.	$P_{pvmin}$	50 Watt
6.	$P_{pvmax}$	540 W
8.	$P_{battmax}$	3400 W

The control module utilizing a state variable oversees the system's entire functioning. It observes both the SOC of the battery and the state of the SC. By considering the system's operational parameters and predetermined limits, the state variable decides whether the battery and SC should be charged or discharged.

#### IV Result and Discussion

The simulation has been carried out on the basis of material and methods for SVC strategy presented in above section and the results of simulation are presented in this section.

The input voltage of the PV array converter exhibits a pattern of peaks and troughs, which correspond to changes in solar irradiance between the operating states of the PV array as controlled by the state variables. Fig. 9 depicts the input voltage curves of the converters for both the PV array and the battery. The PV array converter input voltage varies in response to the irradiance of the PV array. It increases from 0 to 5 seconds, reaching its maximum value of 120 volts at 5 seconds, and then decreases from 120 volts to 0 volts during the time from 5 to 10 seconds. The second curve of the graph displays the voltage of the battery converter. This curve shows the initial battery voltage of 52.2 volts, which remains constant from 0 to 3.5 seconds. After 3.5 seconds, when the battery is operated according to the rules of SVC, the battery graph exhibits voltage drop from 56 volts to 46 volts.

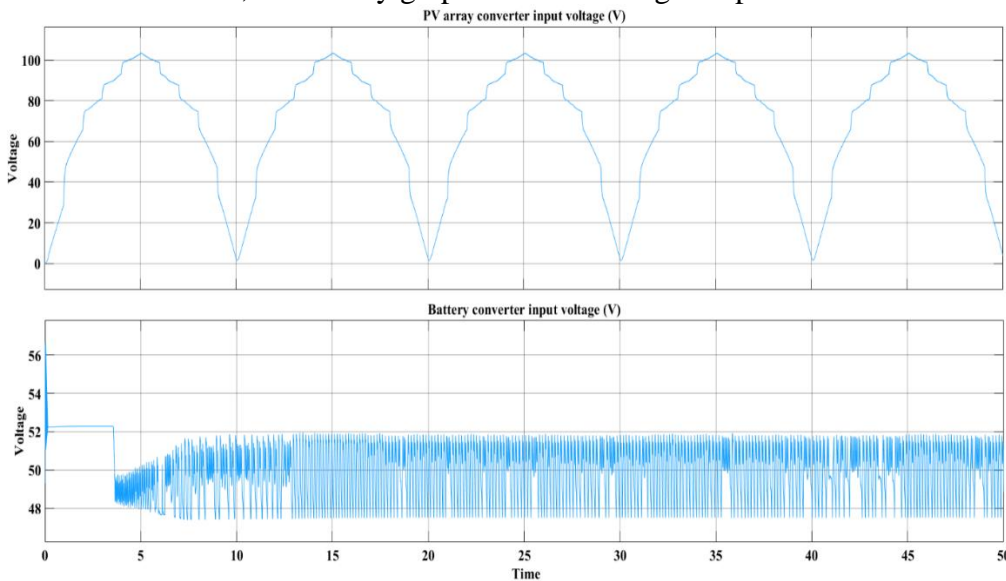


**Fig. 9: PV array and battery converter input voltage curve of SVC.**

The curves in Fig. 10 depicts a few output parameters of Li-ion battery such as current, voltage and SOC segregated into three different plots. The first curve depicts the battery current, the second curve shows the battery voltage, and the third displays the SOC of the battery while feeding the load requirements. It can be observed from the curves that the battery current remains 0 amps from 0 to 3.5 seconds, as it remains non-operational. During this time interval, power is supplied through the PV array and SC. After 3.5 seconds, the load power increases from 1342 to 1354 watts, thus the battery is operated and the value of current gradually increases, as can be observed in the battery current curve in Fig. 10 Simultaneously, the battery voltage decreases from 52.5 to 51.5 volts. Initially, the battery SOC is 65%, and it gradually decreases from 65% to 64.3% during the time interval of 0 to 50 seconds.

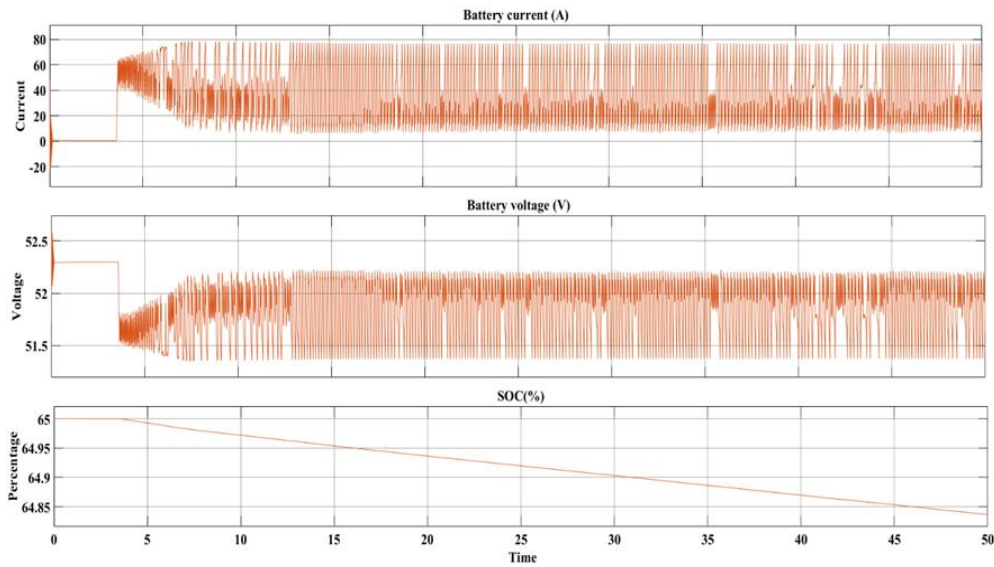


**Fig. 10: Battery current, voltage, and SOC curves of SVC.**

Fig.11 shows the SC following the initial discharge, both the current and voltage graphs exhibit a pattern of small, fast oscillations. This behavior suggests that the SC is frequently engaging and disengaging to smooth out rapid changes in power demand or supply, a common role for supercapacitors in EMS. The graph indicates that the SC voltage decreases from 269 volt to 267.8 volt and current changes from 2 to 10 amperes during time interval of 0 to 3.5 second. SC current exhibit deviations from  $-5$  to  $+5$  ampere and voltage from 269 volts to 271 volts during the time interval of 3.5 sec to 50 seconds.

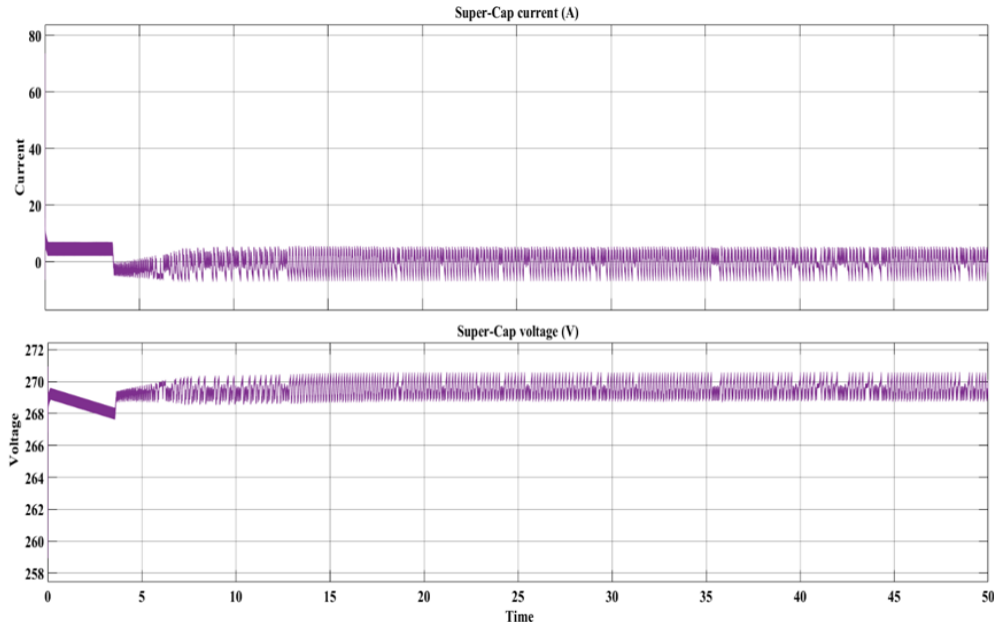


**Fig. 11: SC current, voltage curve of SVC.**

From Fig. 12, it is evident that the power management between the load, PV array, battery, and SC over a time span of 50 seconds is done effectively using the proposed SVC.

As per the rules of SVC in Table 7, if the SOC of the battery is high and the load power requirement exceeds the minimum value of PV power  $P(P_{pvmin,})$  then the PV power should be less than the minimum value of PV power. This condition is satisfied by the power curve shown in Fig. 12. At 0.5 seconds, the SOC is 65%, the PV power is 12 watts, and the load power is 670 watts, which exceeds the minimum PV power. State 2 is also satisfied by this graph at 4 seconds, the SOC is 65%, and the load power is 1770 watts, which exceeds the maximum value of PV power, and the PV power 450

watt is greater than the operating power 250 watt of PV array. Similarly, all other rules in the state variable control strategy are followed and the power from the PV array, battery and SC are regulated in accordance with the rules. The power output of the PV array, battery, and SC shows variability, with the SC frequently responding to more immediate fluctuations. This is typical of a state variable approach where the system switches between different modes of operation (charging, discharging) based on the load requirements and the state of the energy sources.

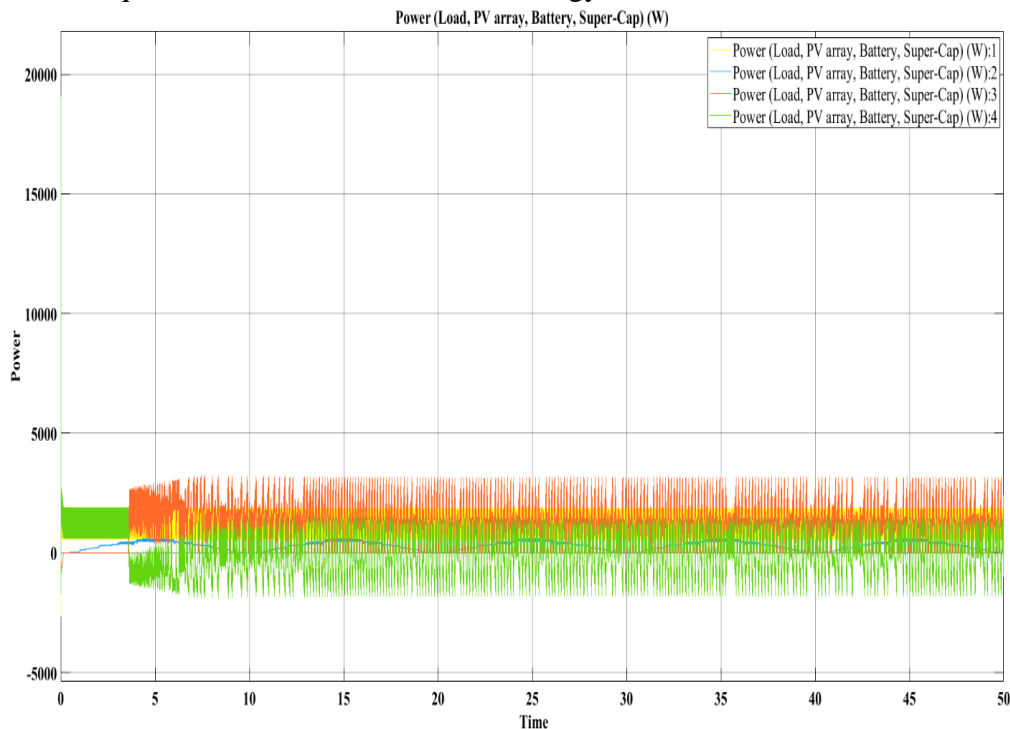


**Fig. 12: Power curve of load, PV array, battery, SC in SVC.**

Overall, the SVC in these graphs is characterized by its distinct operational states, which shows the subsequent transitions to different power levels. The approach effectively manages the interactions between the PV array, battery, and SC to provide a stable power supply to the load. The use of the SC for immediate response and the battery for longer-term energy balance is evident, and the variability in the converter input voltages indicates active management of both energy generation and storage components.

## V. Conclusion

In this research work, a thorough analysis of EMS using SVC is presented. The benefits of the EMS are presented and verified, systematically through simulation. In the SVC, discrete operational states are evident, managing distribution of power into the load emanating from PV array, battery, and supercapacitor. Specific focus was given to graphs illustrating power distribution, battery metrics, supercapacitor performance, and converter input voltages. The strategy demonstrated effective management of energy sources and was capable of providing stable power to the load, with the SC responding and mitigating the immediate fluctuations in the load requirements.

## References

[1] **Smith, D., Douglas, R. and Naeem, W., 2018.** Fuzzy rule-based energy management strategy for a parallel mild-hybrid electric bus. In *2018 IEEE International Conference on Electrical Systems for Aircraft, Railway, Ship Propulsion and Road Vehicles & International Transportation Electrification Conference (ESARS-ITEC)* (pp. 1-5). IEEE.

[2] **Alloui, H., Khoucha, F., Rizoug, N., Benbouzid, M. and Kheloui, A., 2017.** Comparative study between rule-based and frequency separation energy management strategies within fuel-cell/battery



electric vehicle. In *2017 IEEE International Conference on Environment and Electrical Engineering and 2017 IEEE Industrial and Commercial Power Systems Europe (EEEIC/I&CPS Europe)* (pp. 1-5). IEEE.

[3] **Aouzellag, H., Abdellaoui, H., Iffouzar, K. and Ghedamsi, K., 2015.** Model-based energy management strategy for hybrid electric vehicle. In *2015 4th International Conference on Electrical Engineering (ICEE)* (pp. 1-6). IEEE.

[4] **Sankarkumar, R.S. and Natarajan, R., 2021.** Energy management techniques and topologies suitable for hybrid energy storage system powered electric vehicles: An overview. *International Transactions on Electrical Energy Systems*, 31(4), pp. 12819.

[5] **Bahuguna, N.K., and Singh, R., 2023.** Simulation and critical performance evaluation of a two-wheeler EV system under varying aerodynamic and terrain condition. *Ind. Eng. j.*, 52(12): 46-55.

[6] **Choi, M. E., Lee, J. S. and Seo, S. W. 2014.** Real-time optimization for power management systems of a battery/supercapacitor hybrid energy storage system in electric vehicles. *IEEE Trans. Veh. Technol.*, 63(8):360-3611.

[7] **Dusmez, S. and Khaligh, A. 2014.** A supervisory power-splitting approach for a new ultracapacitor-battery vehicle deploying two propulsion machines. *IEEE Trans. on Ind. Inf.*, 10(3):1960-1971.

[8] **Ehsani, M., Rahman, K.M. and Toliyat, H.A., 1997.** Propulsion system design of electric and hybrid vehicles. *IEEE Trans. on ind. Elect.*, 44(1):19-27.